Applied Surface Science 736 (2026) 166749

Contents lists available at ScienceDirect

Applied Surface Science

journal homepage: www.elsevier.com/locate/apsusc

Full Length Article

Substituent effects on catechol adhesion and interfacial electronic interactions on graphite: a DFT study

Mengdi Zhao [a,1], Jinjin Zhang [a,1], Yanhong Yin [a], Chunxian Guo [a,*], Joonkyung Jang [b,*]

[a] Department of Materials Science and Engineering, Suzhou University of Science and Technology, Suzhou 215009, PR China
[b] Department of Nanoenergy Engineering, Pusan National University, Busan 46241, the Republic of Korea

ARTICLE INFO

Keywords:
Catechol derivatives
Density functional theory
Bioinspired adhesion
Interfacial charge transfer
Functional group modulation

ABSTRACT

This study investigates the adhesion of catechol and its derivatives to graphite to elucidate the effects of chemical functionalization and molecular flexibility on adhesion. Density functional theory (DFT) was used to systematically examine various electron-donating and electron-withdrawing substituents. All catechol derivatives exhibited strong adhesion to graphite, confirming the intrinsic adhesive capability of the catechol motif. Multiple substituents on the aromatic ring of catechol did not provide further improvement beyond that achieved by the strongest single substituent. In contrast, attachment of a flexible aliphatic chain with a polar end group markedly increased adhesion strength by enabling multipoint contact with the surface. Electron-donating substituents tend to increase electron density on the adsorbed molecule relative to the graphite surface. In contrast, electron-withdrawing substituents lead to the opposite redistribution of electron density, with a slight depletion of electron density on the molecule relative to graphite. The calculated adsorption energies indicate that catechol derivatives bearing electron-withdrawing substituents generally exhibit stronger adsorption on graphite than those containing electron-donating groups. The direction and magnitude of interfacial electron redistribution correlate with the electronic structure of the substituent and the resulting adhesion strength. This study provides useful guidelines for the rational design of bioinspired catecholic adhesives and coatings.

1. Introduction

Marine mussels adhere robustly to wet surfaces, even under conditions of high salinity and dynamic flow. Mussels secrete byssal adhesive proteins that enable firm attachment to rocks, ship hulls, and various submerged surfaces despite relentless wave action [1–3]. *Mussel foot proteins* (Mfps) are unusually rich in the L-3,4-dihydroxyphenylalanine (DOPA) residue. The catechol group of DOPA forms strong bidentate interactions with surface oxides through hydrogen bonding and metal coordination, thereby significantly enhancing adhesion to metal oxide substrates (e.g. Al_2O_3) [4–6]. DOPA also coordinates metal ions such as Fe^{3+}, V^{3+}, and Al^{3+} to form stable tris-catecholate complexes [7–9], which further contribute to robust wet adhesion on oxide-containing surfaces [1,10]. Beyond metal coordination, Mfps employ diverse non-covalent interactions to adhere to a wide range of substrates. Mussels can form underwater bonds with materials including glass, plastics, and metal oxides [11]. These adhesive interactions arise from a combination of mechanisms, including bidentate hydrogen bonding to polar surfaces, hydrophobic and van der Waals interactions with nonpolar substrates, and cation–π interactions involving positively charged residues [12,13]. In addition, aromatic residues such as DOPA can interact favorably with π-electron-rich or hydrophobic surfaces through dispersive and π-related interactions, contributing to adhesion on carbonaceous and polymeric materials. Collectively, these interactions enable Mfps to adhere strongly to both soft and hard surfaces and to both polar and nonpolar substrates under wet conditions [14,15], as schematically illustrated in Fig. 1.

Graphite is a prototypical hydrophobic material with a layered structure and an extended π-electron system. Investigating the adhesion of catechol and its derivatives to this substrate is therefore of particular interest. Compared with a single graphene sheet, multilayer graphite more closely represents real engineered surfaces and provides a tunable interfacial environment for molecular immobilization, charge transfer, and energy dissipation. The electronic band structure and surface states of graphite differ from those of isolated graphene, which can influence the adsorption behavior of catechol-like molecules. These characteristics

* Corresponding authors.
E-mail addresses: cxguo@usts.edu.cn (C. Guo), jkjang@pusan.ac.kr (J. Jang).
[1] Co-first authors with equal contribution.

https://doi.org/10.1016/j.apsusc.2026.166749
Received 26 January 2026; Received in revised form 18 March 2026; Accepted 28 March 2026
Available online 30 March 2026

have motivated interest in graphite for applications ranging from anti-fouling coatings to nanoelectronics and biosensors. Previous theoretical studies have explored molecular adsorption and adhesion on graphitic carbon surfaces, emphasizing the role of dispersion interactions and π–π stacking in stabilizing molecule–surface interfaces. For example, first-principles calculations have been used to examine the adhesion of epoxy resin fragments on graphite and hexagonal boron nitride surfaces, showing that the interaction with graphite is mainly governed by dispersion forces between aromatic rings and the graphitic basal plane [16]. Other studies have investigated the adsorption of phenolic molecules on graphene-based materials and found that aromatic stacking and functional groups can significantly affect adsorption strength and interfacial charge transfer [17].

Despite these efforts, current understanding of molecular adhesion on graphite remains incomplete. Most previous studies have focused on idealized graphene sheets or functionalized graphene oxide surfaces, while relatively few studies have systematically examined how different molecular functionalizations and substituents influence adsorption behavior on layered graphite surfaces. In particular, the detailed adhesion mechanisms of catechol-based adhesive molecules on graphite are not fully understood, especially with respect to how different molecular functionalizations influence adsorption strength and interfacial electronic structure.

One promising strategy to tune the adhesion of catechol to carbon surfaces is to modify the aromatic ring with various substituents. Simulation studies have shown that both electron-donating and electron-withdrawing substituents on the aromatic ring can enhance adhesion to graphene, with polar groups such as hydroxyl (–OH) exerting particularly strong effects [18]. In addition, first-principles investigations of layered graphite surfaces have revealed that strong electron-withdrawing substituents can markedly strengthen adsorption by enhancing π–π interactions and interfacial charge transfer between catechol derivatives and the carbon surface [19]. Increasing the number of –OH groups on a phenylene ring (i.e., increased ring hydroxylation) significantly enhances adsorption affinity, whereas the specific arrangement of these –OH groups (ortho vs. para) plays a comparatively minor role [20]. Consistent with these findings, introducing polar functional groups on carbon adsorbents can strengthen adsorption through specific interactions; for example, carboxyl (–COOH) groups on carbon surfaces can form strong hydrogen bonds with phenolic –OH groups of adsorbates, thereby improving phenol uptake [21,22]. Furthermore, molecules with similar structures can exhibit distinct adsorption preferences depending on their functional groups. For instance, catechol (with vicinal dihydroxyl groups) and aniline (with an $–NH_2$ group) show different adsorption affinities for epoxy versus carboxyl sites on graphene oxide, underscoring the complex interplay between molecular functional group chemistry and surface functionality [19,23].

At present, theoretical studies examining how functional group chemistry, substituent positioning, and molecular flexibility collectively influence the adhesion of catechol to graphite are scarce. Previous work has typically focused on varying only a single parameter, such as evaluating the effect of an individual substituent on pristine graphene [24] or examining adsorption behavior on oxidized carbon surfaces with fixed functionalities [19]. This gap highlights the need for a comprehensive study that explores potential synergistic effects or trade-offs among multiple substituents, as well as the role of flexible linkers in modulating adhesion strength, interfacial conformation, and charge

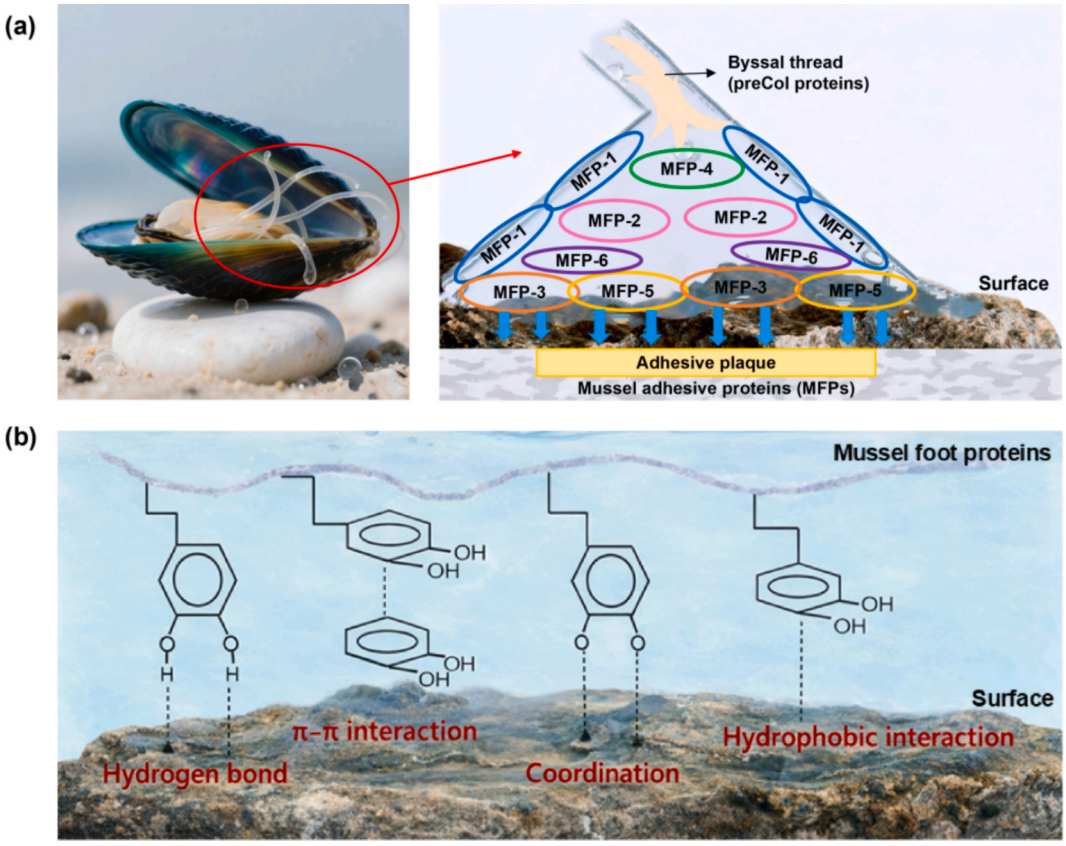

Fig. 1. Mussel-inspired wet adhesion mechanisms. (a) Photograph of a mussel attached to a substrate via byssal threads (left) and a schematic illustration of the adhesive plaque formed by major mussel foot proteins (Mfp-1 to Mfp-6) at the substrate interface (right). These proteins collectively contribute to underwater adhesion. (b) Catechol moiety of DOPA enables adhesion through multiple interaction modes with different substrate surfaces, including hydrogen bonding and metal coordination on oxide surfaces, hydrophobic and van der Waals interactions on nonpolar materials, as well as π-related or cation-π interactions that facilitate adhesion to carbonaceous or polymeric substrates.

transfer of catechol. Addressing these aspects is essential for bridging molecular-level design with macroscopic performance, particularly in the development of bioinspired adhesives that function across diverse material classes and in the engineering of surface coatings with tailored adhesion and electronic properties.

Herein, we address these knowledge gaps through first-principles density functional theory (DFT) calculations. We systematically analyze the adsorption of catechol-based molecules on a graphite surface. A wide range of catechol derivatives is considered, including molecules with single-ring substituents (–NH_2, –COOH, –OH, –NO_2, –CF_3, –CH_3, –CN) in both ortho and para positions relative to the hydroxyl groups of catechol, as well as a di-substituted catechol bearing both –NH_2 and –COOH. To examine the role of molecular flexibility, catechol derivatives with aliphatic linkers terminated with –COOH are also evaluated, specifically catechol–CH_2–COOH, catechol–$(CH_2)_2$–COOH, and catechol–$(CH_2)_3$–COOH, with the chain attached at the 4-position of catechol, opposite one of the native –OH groups. For each molecule, key interfacial properties are computed, including adsorption energy, optimized adsorption geometry, and interfacial charge transfer. The results reveal how substituent identity, electronic properties, and chain flexibility influence π–π interactions and charge redistribution at the interface. These insights provide a coherent molecular-level understanding of catechol adhesion on carbon surfaces and offer theoretical guidance for designing high-performance adhesives, electrochemical interfaces, and other functional coatings based on catechol-derived molecules.

2. Computational methods

DFT calculations were performed to investigate the adsorption of catechol and its derivatives on a graphite surface [25,26]. All calculations were carried out using the Vienna Ab initio Simulation Package (VASP) [27,28]. The Perdew–Burke–Ernzerhof (PBE) generalized gradient approximation functional [29,30] was employed to describe exchange–correlation effects. Dispersion interactions were included using the DFT-D3 dispersion correction implemented in VASP to account for long-range van der Waals interactions between the adsorbate and the graphite surface. Core-valence interactions were treated using the projector augmented-wave (PAW) method, and a plane-wave basis set with a kinetic energy cutoff of 450 eV was applied.

The graphite substrate was modeled as an AB-stacked multilayer graphene slab within a periodic supercell. A 6 × 6 lateral supercell containing 144 carbon atoms was used, with lattice parameters of approximately 14.76 Å in both the x and y directions. After structural optimization, the interlayer spacing of graphite was 3.37 Å and the C–C bond length was 1.42 Å, in close agreement with experimental and previous theoretical values [31–33]. A vacuum region of 25 Å was applied perpendicular to the surface to prevent spurious interactions between periodic images. The slab model included a single exposed graphite basal plane for adsorption; the bottom graphene layer was fixed at bulk positions during relaxation, while the upper layers and the adsorbate were fully relaxed. Brillouin zone sampling was performed using a Gamma-centered k-point grid, which was sufficient to ensure total-energy convergence given the large supercell size. The electronic self-consistent field convergence criterion was set to 1×10^{-5} eV, and structural optimizations were considered converged when the residual forces on all atoms were below 1×10^{-4} eV $Å^{-1}$.

A series of catechol-based adsorbate molecules was constructed, with catechol (1,2-dihydroxybenzene) serving as the base molecule. Chemical analogues of catechol bearing single substituents (–NH_2, –COOH, –OH, –NO_2, –CF_3, –CH_3, and –CN) on the phenylene ring were then considered. For each substituent, two regioisomeric configurations were modeled: one with the substituent in the ortho position (adjacent to a catechol –OH group) and one in the para position (opposite a –OH group). A di-substituted catechol carrying both an –NH_2 and an –COOH group on the ring, combining a strong electron donor and a strong electron-withdrawing group on the same aromatic ring, was also examined. In addition, three derivatives with flexible alkyl linkers were investigated: catechol–CH_2–COOH, catechol–$(CH_2)_2$–COOH, and catechol–$(CH_2)_3$–COOH. In these molecules, a carboxylic acid functional group is attached to the catechol ring via an aliphatic chain of one, two, or three methylene units, with the chain connected at the 4-position of catechol, opposite one of the native –OH groups. The molecular structures considered in this study are illustrated in Fig. 2. For several representative systems, different initial adsorption geometries were tested to confirm the stability of the optimized adsorption configuration.

Adsorption energies (E_{ads}) were calculated to quantify the strength of molecule–surface interactions. The adsorption energy is defined as follows:

$$E_{ads} = E_{total} - (E_{slab} + E_{molecule}),$$

where E_{total} is the DFT total energy of the optimized adsorbed system, E_{slab} is the energy of the isolated graphite slab, and $E_{molecule}$ is the energy of the isolated molecule in the same cell (with slab and molecule geometries fixed as in the adsorbed state). A negative E_{ads} indicates an exothermic (favorable) adsorption.

To analyze electronic interactions at the interface, Bader charge analysis was performed on the charge density of each optimized adsorption system. This allowed estimation of the net charge transfer between the molecule and graphite upon adsorption. Charge transfer values are reported as Δq (in units of electrons), defined such that a positive Δq indicates electron gain by the molecule (and equivalent electron loss by the surface), whereas a negative Δq indicates electron transfer from the molecule to the surface. Additionally, charge density difference maps were generated to visualize electron redistribution upon adsorption. The differential charge density is defined as

$$\Delta\rho(\mathbf{r}) = \rho_{(\text{molecule+surface})}(\mathbf{r}) - [\rho_{(\text{molecule})}(\mathbf{r}) + \rho_{(\text{surface})}(\mathbf{r})],$$

and was plotted as isosurfaces, with regions of electron accumulation and depletion indicated by different colors, to qualitatively illustrate donor–acceptor charge redistribution at the interface. All structural and charge-density visualizations were prepared using VESTA and related software.

3. Results and discussion

3.1. Adsorption energies of catechol and its derivatives

All catechol-based molecules investigated in this study exhibited strong adsorption on the basal plane of graphite. For the parent catechol molecule (1,2-dihydroxybenzene) without additional substituents, the calculated adsorption energy was approximately –55 kJ·mol^{-1}. This result confirms that the catechol dihydroxyl motif possesses an intrinsic affinity for π-electron-rich carbon surfaces, likely through π–π stacking of its aromatic ring on the graphite lattice, complemented by dispersive van der Waals interactions.

Introducing electron-donating groups, such as –NH_2 and –CH_3, significantly enhanced adsorption strength compared with catechol. As shown in Fig. 3, these substituents consistently yielded stronger adsorption in para configurations than in ortho, typically by 1–3 kJ·mol^{-1}. For instance, amino-substituted catechol exhibited $E_{ads} \approx -67.5$kJ·mol^{-1} in the ortho configuration and –70.3 kJ·mol^{-1} in the para configuration. Similarly, methyl-substituted catechol showed $E_{ads} \approx$ –63.0 kJ·mol^{-1} (ortho) and –64.2 kJ·mol^{-1} (para). Compared with catechol (approximately –55 kJ·mol^{-1}), these results indicate that adding an electron-donating group can strengthen the molecule–graphite interaction by roughly 8–15 kJ·mol^{-1}. Mechanistically, electron-donating substituents enrich the electron density—and thus the polarizability—of the aromatic ring, which likely enhances π–π dispersion interactions with graphite and can induce favorable dipole–induced-dipole interactions. Among the donors tested, –NH_2, a strong

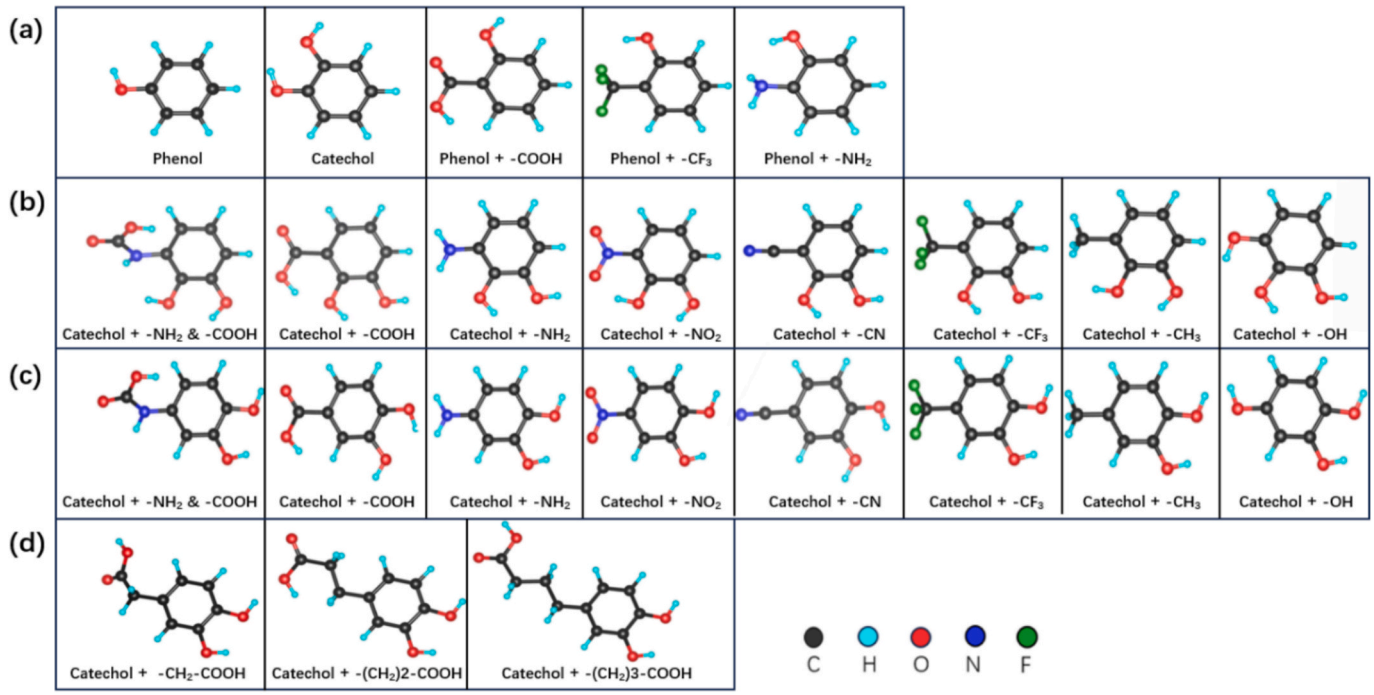

Fig. 2. Molecules investigated: (a) catechol and phenol as reference molecules; (b) ortho-substituted catechol derivatives (–NH_2–COOH, –COOH, –NH_2, etc.); (c) para-substituted catechol derivatives; (d) catechol derivatives with flexible alkyl chains terminated with –COOH.

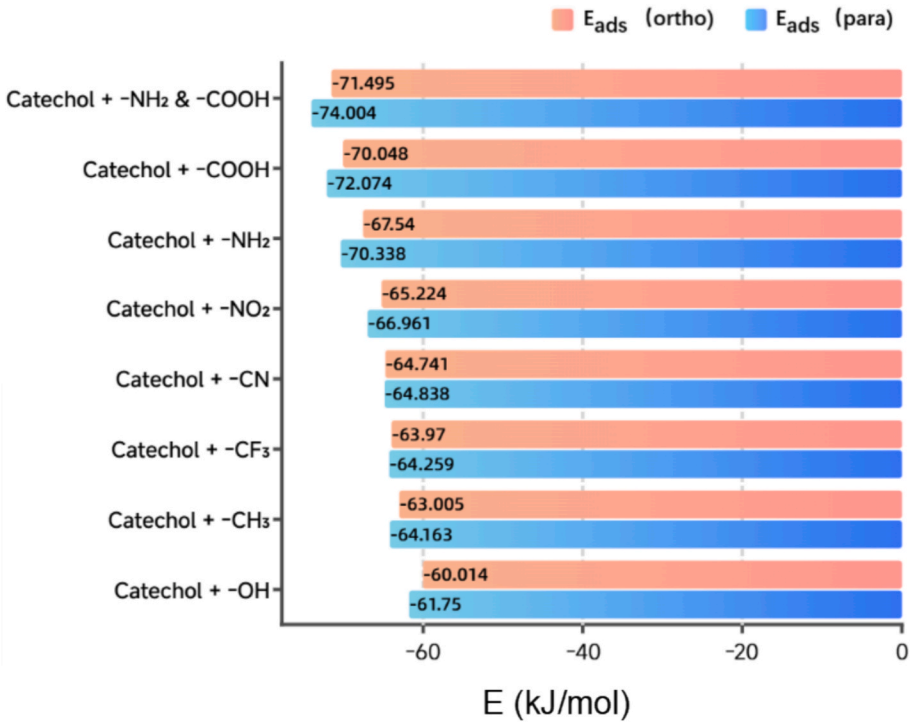

Fig. 3. Comparison of adsorption energies for ortho- and para-substituted catechol derivatives.

electron-releasing substituent via resonance, produced one of the largest increases in adsorption. This finding aligns with experimental observations that poly(catecholamine) coatings, rich in amine-bearing catechol units, adhere well to carbon surfaces and agrees with prior simulations showing that aromatic amines bind strongly to graphene-based materials [34–36].

Electron-withdrawing (EW) substituents, such as –NO_2, –CF_3, –CN, and –COOH, were also found to enhance adsorption on graphite relative to unsubstituted catechol, although the magnitude of the effect varied by group. For example, nitro-substituted catechol exhibited $E_{ads} \approx$ –65.2 kJ·mol^{-1} for the ortho isomer and –67.0 kJ·mol^{-1} for the para isomer. The cyano (–CN) and trifluoromethyl (–CF_3) substituents produced more moderate enhancements, with adsorption energies around –63 to –65 kJ·mol^{-1}. Notably, carboxyl-substituted catechol (–COOH) showed very strong adsorption, with $E_{ads} \approx$ –70.0 kJ·mol^{-1} in the ortho configuration and –72.1 kJ·mol^{-1} in the para configuration, nearly matching the

enhancement observed for –NH_2. The pronounced effect of the –COOH group likely arises from its dual character. While –COOH withdraws electron density from the aromatic ring, it can also engage in additional interactions. For instance, an ortho –COOH can form an intramolecular hydrogen bond with a neighboring –OH group, and the polar –COOH increases the overall molecular dipole moment, which can induce complementary image charges on the graphite surface, strengthening adsorption. Although graphite does not provide specific hydrogen-bonding sites, polar functional groups on the adsorbate can polarize the π-electron cloud, enhancing physisorption. This observation of –COOH's effectiveness is consistent with previous studies of phenolic adsorption on functionalized carbons, which reported that carboxyl groups can strongly anchor adsorbates via specific interactions such as hydrogen bonding [37,38].

Fig. 4 further illustrates relative adsorption strengths by comparing E_{ads} values for phenol, catechol, and three representative phenol derivatives functionalized with –CF_3, –NH_2, and –COOH. The figure highlights that –NH_2 and –COOH substitutions produce the most significant enhancements. These trends align with prior simulation studies [18], reinforcing the conclusion that the electronic nature of the substituent is the primary determinant of adsorption strength, while regiochemistry (ortho vs. para) plays a secondary role.

Experimental observations on catechol-based surface functionalization provide useful support for the substituent-dependent interactions identified here. Catechol-containing molecules and coatings such as polydopamine are known to adhere strongly to carbon-based materials, including carbon fibers and graphitic surfaces [39,40]. In these systems, catechol and amine functionalities contribute to interfacial binding through a combination of π–π interactions, hydrogen bonding, and donor–acceptor interactions at the carbon interface [39]. In addition, surface functionalization with polar groups such as amine or carboxyl groups has been reported to enhance interfacial adhesion in carbon-based composite systems by modifying interfacial polarity and molecular interactions near the carbon surface [40]. These experimental observations are consistent with the present DFT results, which show that substituent identity can significantly influence adsorption on graphite through electronic effects and interfacial charge redistribution.

Interestingly, the addition of a third hydroxyl group to the aromatic ring (forming a tri-hydroxylated benzene) results in only a modest increase in adsorption strength (approximately 5–7 kJ·mol^{-1} compared with catechol), indicating diminishing returns beyond the two hydroxyl groups of the catechol motif. This underscores the inherent effectiveness of the catechol diol motif, a feature similarly exploited in mussel adhesive chemistry through the two vicinal –OH groups of DOPA [6,41–43].

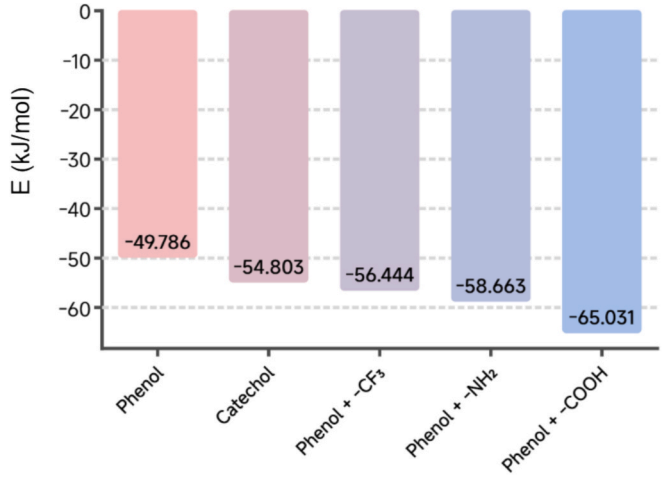

Fig. 4. Adsorption energies of catechol, phenol, and selected phenol derivatives.

3.2. Synergistic effects of multiple substituents and flexible chains

Having established the effects of individual ring substituents, we next examined molecules bearing multiple functional groups, as well as cases in which a substituent is attached via a flexible linker. First, a di-substituted catechol carrying both an –NH_2 and a –COOH group on the ring, combining a strong electron donor and a strong electron-withdrawing group, was considered. One might expect such a dual-functional molecule to exhibit additive or synergistic adsorption effects. However, our calculations indicate otherwise: the adsorption energies for the dual-substituted catechol were $E_{ads} \approx -71.5$ kJ·mol^{-1} for one configuration (–NH_2 ortho and –COOH para to the catechol –OH groups) and –74.0 kJ·mol^{-1} for another isomer (both –NH_2 and –COOH in para positions relative to the dihydroxyls). These values are comparable to those of the strongest single-substituent cases, nearly matching the E_{ads} obtained for catechol with either –NH_2 or –COOH alone. In other words, combining a donor and an acceptor on the same aromatic ring did not yield a significantly higher adsorption energy than that achieved by a single substituent. This suggests that the effect of a strong substituent on the aromatic π-system saturates the adsorption enhancement: once the electron distribution of the ring is substantially polarized or altered by one group, the addition of a second functional group provides diminishing returns. Moreover, in the ortho configuration, –NH_2 and –COOH can form an intramolecular hydrogen bond, potentially reducing their ability to independently interact with the surface. Thus, a single well-chosen substituent—either a strong donor or a strong acceptor—appears sufficient to achieve most of the possible adhesion gain on graphite, and adding additional functional groups on the same ring does not linearly increase adsorption strength.

An alternative strategy to further enhance adhesion is to attach a functional group via a flexible aliphatic tether, effectively providing the molecule with multiple contact points on the surface. This was explored by appending carboxylic acid–terminated alkyl chains of varying lengths to the catechol ring. Specifically, catechol–CH_2–COOH, catechol–$(CH_2)_2$–COOH, and catechol–$(CH_2)_3$–COOH were tested, with the chain attached at the ring position opposite one of the catechol –OH groups. The calculated adsorption energies (Fig. 5) show a remarkable increase with chain length. Adding a single –CH_2–COOH substituent (one methylene linker) yielded $E_{ads} \approx$ –64.6kJ·mol^{-1}, a modest improvement over catechol. Extending the linker to two methylene units, –$(CH_2)_2$–COOH, led to $E_{ads} \approx$ –86.5kJ·mol^{-1}. With three methylene units (catechol–$(CH_2)_3$–COOH), the adsorption energy reached $E_{ads} \approx$ –89.9kJ·mol^{-1}. The longest chain thus nearly doubled the adsorption energy compared with unsubstituted catechol (approximately –90 kJ·mol^{-1} vs. approximately –55 kJ·mol^{-1}). To our knowledge, this represents the strongest adsorption energy obtained for any molecule in this study.

The dramatic increase in adsorption energy observed when extending from one to two methylene units (>20 kJ·mol^{-1}) suggests that a

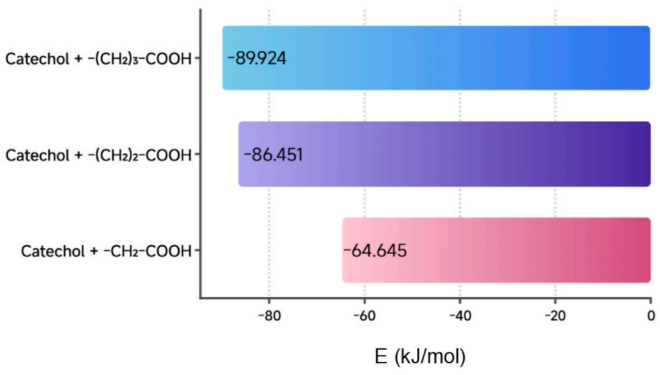

Fig. 5. Adsorption energies of the carboxyl-terminated alkyl chain length series.

single –CH_2–COOH is too short to allow the carboxyl group to effectively engage the surface in addition to the aromatic ring. By contrast, the –$(CH_2)_2$–COOH and –$(CH_2)_3$–COOH chains are long enough to bend and lie along the graphite surface alongside the catechol ring. In the optimized geometries, the catechol ring adsorbs flat against the graphite, maximizing π–π overlap, while the flexible alkyl chain also rests nearly flat, allowing its methylene segments to make van der Waals contacts with the surface. Essentially, the longer alkyl chain provides an extended footprint that increases the total contact area with the substrate beyond that of the aromatic ring alone. The increase in E_{ads} from two to three methylene units is smaller (~3.5 kJ·mol^{-1}), indicating a saturation effect: beyond a certain chain length, the entire chain can already be accommodated on the surface, and further extension yields only marginal additional dispersion interactions. Notably, the terminal –COOH group in these systems does not directly bond to the inert graphitic surface, but it may contribute by stabilizing the adsorbed conformation, for example through intramolecular hydrogen bonding to the catechol –OH, as observed in some optimized structures. In a realistic wet environment, a polar end group like –COOH could also interact with interfacial water molecules or ions, while the hydrophobic portion of the molecule adheres to the surface. However, our vacuum-phase calculations isolate the intrinsic effect of the flexible tail itself.

These findings demonstrate that incorporating a flexible linker can synergistically enhance adhesion by enabling multi-point contact. The rigid aromatic core provides strong π–π anchoring, while the attached alkyl chain contributes additional van der Waals interactions. Among all modifications tested, the combination of an aromatic ring with a flexible aliphatic "tail" produced the highest overall adhesion. From a bio-inspired design perspective, this suggests that an adhesive molecule or polymer containing both aromatic (catechol) units and hydrophobic flexible segments could achieve particularly high affinity for hydrophobic surfaces such as graphite. Indeed, some mussel adhesive proteins contain hydrophobic domains alongside DOPA residues [44,45], a structural feature likely promoting this type of dual-mode adhesion—π–π stacking combined with dispersive contacts. More broadly, our results indicate that while chemical functionalization of the aromatic ring can tune adhesion to some extent, adding a long, flexible tail can exploit physical interactions to achieve adhesion far exceeding that obtainable through ring chemistry alone.

3.3. Interfacial charge transfer and electronic structure

In addition to adsorption energies, our DFT simulations provide insights into the electronic interactions at the molecule–graphite interface. The Bader charge analysis results for each system are summarized in Table 1, reporting the net charge gained by the adsorbed molecule from the surface (Δq). A striking observation is that the sign of the charge transfer correlates with the substituent's electron-donating or electron-withdrawing character. Catechol derivatives with electron-donating substituents (–NH_2, –CH_3, –OH) exhibit positive Δq values, indicating that the molecule gains electron density upon adsorption (i.e., electrons flow from graphite into the molecule). In contrast, derivatives with electron-withdrawing substituents (–NO_2, –CF_3, –CN, –COOH) display negative Δq values, meaning that the molecule loses electron density to the graphite (electrons flow from the molecule into the surface). For example, –NH_2 catechol shows $\Delta q \approx +0.020$ |e| in the ortho position, and $\Delta q \approx +0.026$ |e| in the para position, indicating that approximately 0.02 electrons (ortho) and 0.03 electrons (para) are transferred from the surface to the molecule. Conversely, –NO_2 catechol exhibits $\Delta q \approx -0.017$ |e| in the ortho position and $\Delta q \approx -0.022$ |e| in the para position, indicating electron transfer from the molecule to the surface. This behavior aligns with chemical intuition. Electron-donating groups increase the electron density of the molecule's π-system, leading to a small redistribution of electron density at the molecule-graphite interface rather than a complete transfer of electrons into specific molecular orbitals. Conversely, electron-withdrawing groups decrease the electron density of the aromatic ring, creating electron-deficient regions that induce the opposite interfacial polarization, with a slight depletion of electron density on the molecule relative to the graphite surface.

Significant differences in Δq are observed among specific functional groups. Single –COOH–substituted catechol exhibits a small negative charge transfer ($\Delta q \approx$ –0.012 |e| at the ortho position and –0.011 |e| at the para position), whereas in another case, the Δq values at the ortho and para positions are –0.0203 |e| and –0.006 |e|, indicating electron transfer from the molecule to the graphite surface. As the chain length increases (Table 2), the magnitude of negative charge transfer initially increases (e.g., –CH_2–COOH catechol shows $\Delta q \approx$ –0.008, and –$(CH_2)_2$–COOH catechol shows $\Delta q \approx$ –0.012), suggesting that chain extension enhances electronic coupling with the graphite surface. In the short-to-moderate chain-length regime, the alkyl segment imposes minimal resistance to electron transport, allowing the terminal carboxyl group to maintain strong coupling with the substrate. However, when the chain becomes longer, electronic insulation and orientation effects dominate [46–49]. Long alkyl chains, composed mainly of σ-bonds [50–52] act as insulating barriers that increase the electron tunneling distance and reduce orbital overlap at the interface, consistent with the slightly smaller $|\Delta q| \approx$ –0.007 |e| observed for catechol–$(CH_2)_3$–COOH.

Catechol derivatives with weakly electron-donating groups (–CH_3, –OH) exhibit only small positive charge-transfer values. For example, the –CH_3 substituent produces $\Delta q \approx +0.003$ |e| (ortho) and +0.006 |e| (para), while an additional –OH substituent (forming a tri-hydroxylated ring) gives $\Delta q \approx +0.009$ |e| at both ortho and para positions. For comparison, even reference molecules such as phenol (+0.009 |e|) and catechol (+0.006 |e|) show slight electron gain from the surface, whereas the introduction of strongly electron-withdrawing groups (e.g., –COOH or –CF_3) shifts Δq from positive to negative [53–55]. These trends highlight that substituent effects are a critical factor in modulating the electronic structure at the interface.

It should be noted that absolute Δq values on the order of 0.01–0.02 electrons are relatively large for physisorption and may reflect not only the literal transfer of electrons but also polarization and delocalization of electron density across the interface. The Bader charge partitioning aggregates these effects into a single net value. Substituent influence on charge transfer is determined not only by intrinsic electron-donating or -withdrawing strength but also by factors such as conjugation efficiency, geometry-induced polarization, and the sensitivity of Bader analysis to electron-density topology. Therefore, |Δq| should be interpreted as the cumulative outcome of multiple competing electronic effects rather than a direct measure of substituent strength [56,57]. For example, –CH_3 (a mild donor) on catechol yields $\Delta q \approx +0.003$ |e| (ortho) and +0.006 |e|

Table 1
Bader charge transfer (Δq) for ortho- and para-substituted catechol derivatives adsorbed on graphite.

Molecule (Substituent)	Δq (ortho)	Δq (para)
Catechol + –NH_2 & –COOH (dual)	−0.0203	−0.0064
Catechol + –COOH (carboxyl)	−0.0116	−0.0105
Catechol + –NH_2 (amine)	0.0201	0.0258
Catechol + –NO_2 (nitro)	−0.0224	−0.0165
Catechol + –CN (cyano)	−0.0057	−0.0077
Catechol + -CF_3 (trifluoromethyl)	−0.0148	−0.0082
Catechol + –CH_3 (methyl)	0.0026	0.0064
Catechol + –OH (extra hydroxyl)	0.0088	0.0092

Table 2
Bader charge transfer (Δq) for para-substituted catechol-$(CH_2)_n$-COOH derivatives adsorbed on graphite.

Molecule (Substituent)	Δq(para)
Catechol + –CH_2-COOH	−0.0079
Catechol + –$(CH_2)_2$-COOH	−0.0122
Catechol + –$(CH_2)_3$-COOH	−0.0071

(para), whereas –OH (a moderate donor via resonance) gives + 0.009 |e| at both ortho and para positions. Among electron-withdrawing groups, $–CF_3$ (strong inductive withdrawer) produces $\Delta q \approx –0.015$ |e| (ortho) and –0.008 |e| (para), while –CN (strong withdrawer) yields $\Delta q \approx$ –0.006 |e| (ortho) and –0.008 |e| (para) in one orientation. These results indicate that, for instance, para –CN causes significant polarization, resulting in a net transfer of ~0.008 electrons from the molecule to the graphite surface. Interestingly, long alkyl chain derivatives follow the trend of their terminal group: all $–(CH_2)_n–COOH$ derivatives exhibit negative Δq. This is consistent with their strong adsorption; generally, larger charge transfer (in either direction) reflects stronger electronic coupling between the molecule and the surface. In the case of flexible tails, the polar carboxylate end (protonated in our model) likely attracts some electron density, while the extended chain ensures sufficient contact to facilitate this transfer.

To visualize these charge redistribution phenomena, Fig. 6 shows the differential charge density (Δρ) for a representative electron-donor substituted case (catechol–NH_2) compared to an electron-acceptor case (catechol–NO_2) on graphite. In catechol–NH_2 adsorption, electron accumulation (yellow isosurfaces) is observed around the –NH_2 group and the aromatic ring, with corresponding electron depletion (cyan isosurfaces) in the underlying graphite top layer. This pattern confirms electron transfer from graphite to the molecule, with the graphite π-electrons slightly drawn into the aromatic π system of the adsorbate. In the catechol–NO_2 case, the opposite behavior occurs: electron density is depleted on the molecule, particularly in the ring π system near the –NO_2 group, and accumulated in the graphite beneath, indicating electron flow from the molecule to the surface. Notably, the charge redistribution is delocalized across the contact area rather than highly localized, reflecting the extended nature of π–π interactions. These results highlight graphite's ability to act as an electron reservoir—either donating or accepting electrons depending on the adsorbate's electron-affinity—underscoring the surface's charge-screening and polarization capacity.

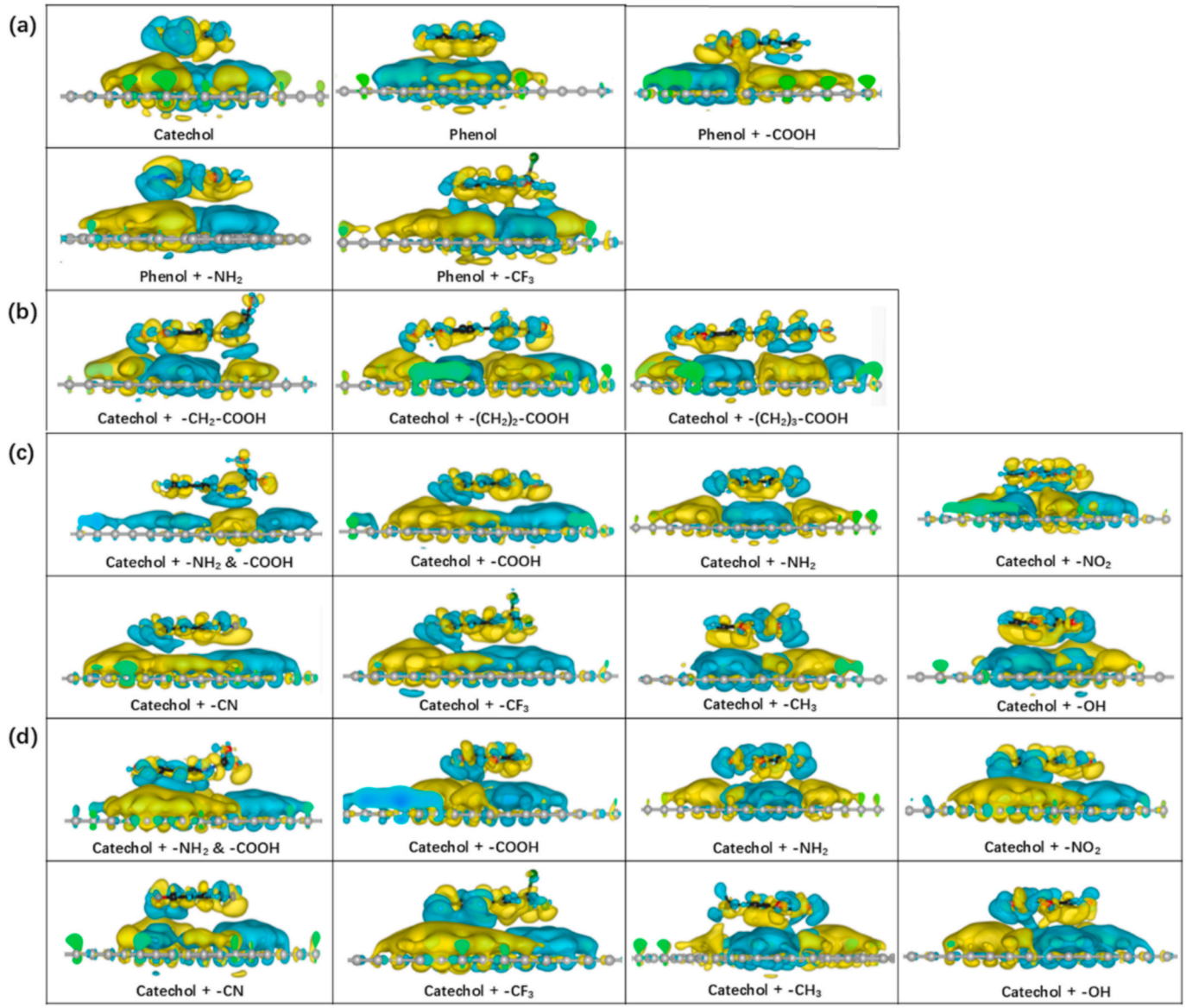

Fig. 6. Differential charge density (Δρ) plots for various catechol-based molecules adsorbed on graphite. Yellow regions indicate electron accumulation; cyan regions indicate electron depletion. (a) Δρ for catechol, phenol, and selected phenol derivatives functionalized with –COOH, –NH_2, and –CF_3; (b) Δρ for catechol derivatives with terminal –COOH groups connected via alkyl chains of increasing length; (c) Δρ for *ortho*-substituted catechol derivatives bearing –NH_2 & –COOH, –COOH, –NH_2, –NO_2, –CN, –CF_3, –CH_3, and –OH; (d) Δρ for the corresponding para-substituted catechol derivatives with the same functional groups as in (c). Differential charge-density isosurfaces were plotted at an isovalue of 6×10^{-5} e $Å^{-3}$.

One notable observation is that, despite the measurable charge transfers, adsorption of these molecules on graphite remains predominantly governed by physical (non-covalent) interactions rather than covalent bond formation. The optimized adsorption geometries (Figs. 7 and 8) show that the molecules remain intact and lie flat, parallel to the graphite surface, at an equilibrium distance of 3.3–3.6 Å, typical for π–π stacking. No evidence of covalent bonding between the adsorbates and the surface was observed. The computed charge redistribution should therefore be interpreted as forming an interfacial dipole. The direction of electron flow establishes a dipole at the interface: for donor-substituted molecules, the adsorbate becomes slightly negatively charged relative to the graphite, whereas the opposite occurs for acceptor-substituted molecules. This asymmetric redistribution of electron density produces an interfacial dipole oriented approximately along the surface normal. Although the magnitude of the charge redistribution is relatively small, it reflects the electronic polarization that accompanies π-π interactions between the aromatic ring and the graphitic surface. Such interfacial dipoles may influence the local electrostatic environment near the surface. In this sense, molecular functionalization provides a way to tune the electronic environment at graphitic interfaces through adsorption-induced electron redistribution.

The observed variations in adsorption strength among substituents can be explained by the interplay of electronic effects and dispersion forces. For example, the $–NH_2$ group enhances adsorption by donating electron density to the aromatic ring via resonance, thereby strengthening π–π interactions with the graphite surface. Similarly, –COOH, a strong electron-withdrawing group, induces significant polarization and charge transfer to the substrate, consistent with its high adsorption energy. In contrast, a nonpolar group such as $–CH_3$ produces minimal electronic perturbation and a correspondingly smaller adsorption

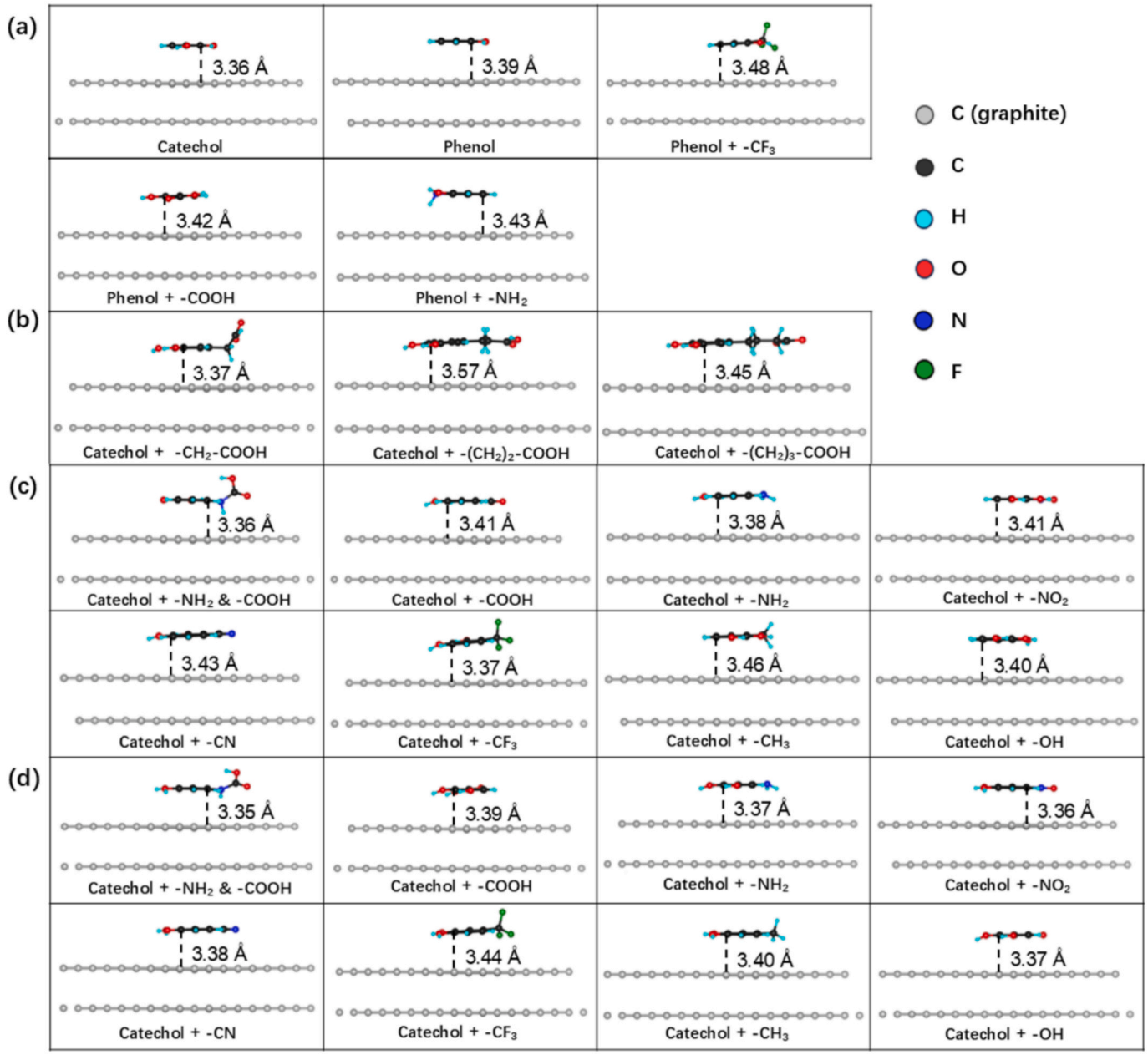

Fig. 7. Side-view snapshots of optimized adsorption geometries for catechol-based molecules on the graphite surface. (a) Catechol, phenol, and representative phenol derivatives functionalized with $–CF_3$, –COOH, and $–NH_2$; (b) Catechol derivatives bearing carboxyl-terminated alkyl chains of varying length; (c) Ortho-substituted catechol derivatives with the following functional groups: $–NH_2$ & –COOH, –COOH, $–NH_2$, $–NO_2$, –CN, $–CF_3$, $–CH_3$, and –OH; (d) Para-substituted catechol derivatives containing the same set of functional groups as in (c).

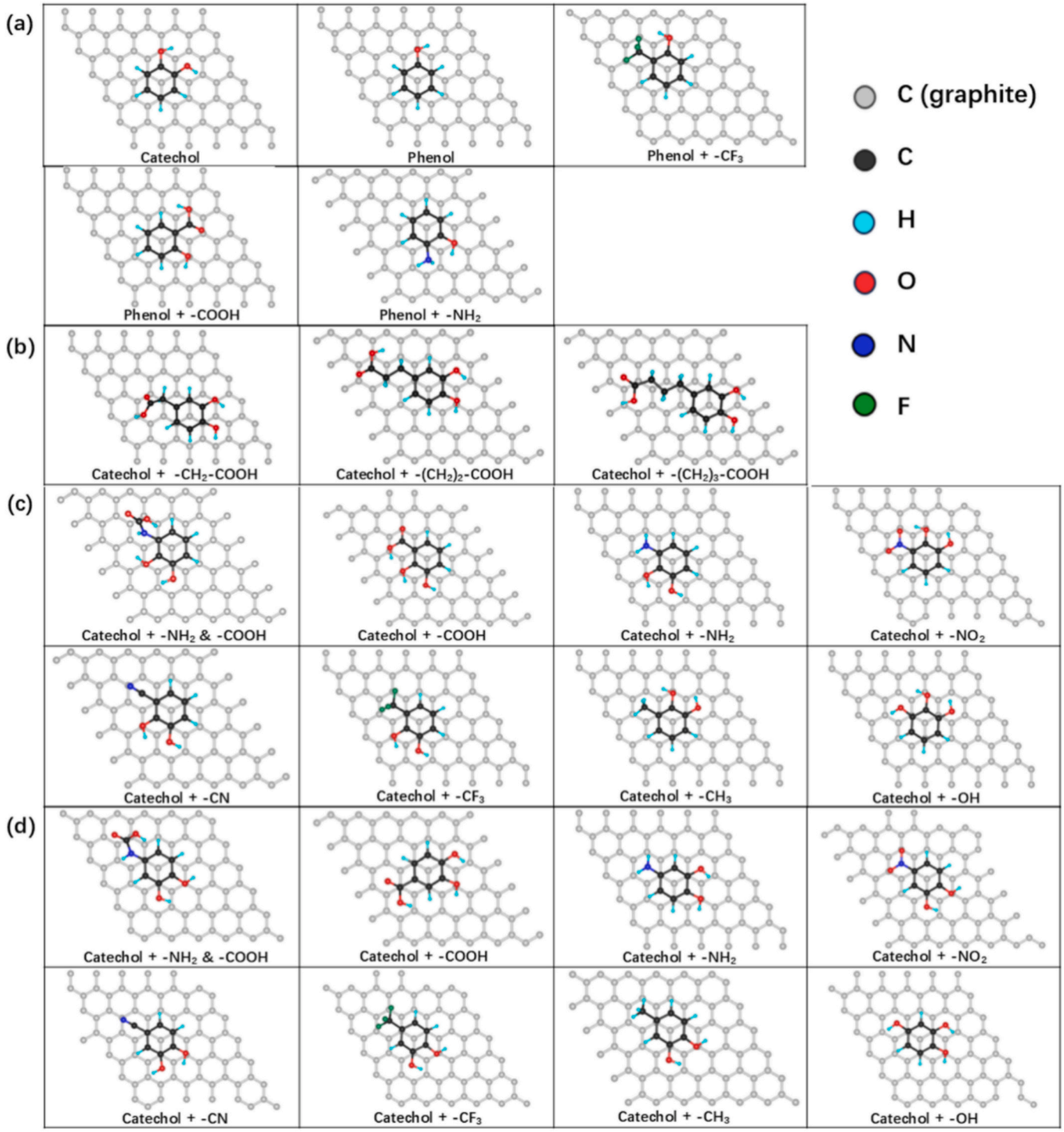

Fig. 8. Top-view snapshots of optimized adsorption geometries for catechol-based molecules on the graphite surface. (a) Catechol, phenol, and representative phenol derivatives functionalized with $-CF_3$, –COOH, and $–NH_2$; (b) Catechol derivatives bearing carboxyl-terminated alkyl chains of varying length; (c) Ortho-substituted catechol derivatives with the following functional groups: $–NH_2$ & –COOH, –COOH, $–NH_2$, $–NO_2$, –CN, $-CF_3$, $–CH_3$, and –OH; (d) Para-substituted catechol derivatives containing the same set of functional groups as in (c).

enhancement, with adsorption dominated by dispersion forces. These results highlight that optimal adhesion arises from a synergy of electronic and van der Waals interactions [44,58]. This principle parallels biological adhesive systems, such as mussel foot proteins, which combine π-stacking catechols with polar or charged functionalities to achieve robust surface attachment.

3.4. Implications for bio-inspired adhesive design

Our theoretical results provide quantitative support and novel insights for designing high-performance bioinspired adhesives and coatings, particularly on carbon-based surfaces. They reinforce experimental observations, such as the strong adhesion of synthetic polymers incorporating catechol to diverse materials [59,60], and indicate that functionalizing catechol with specific substituents can further enhance

adhesion to nonpolar substrates like graphite. The fact that both electron-rich and electron-deficient substitutions improve adsorption mirrors how mussels employ DOPA—which can act as both a hydrogen-bond donor and acceptor and participate in redox or metal-coordination chemistry—together with neighboring residues (e.g., positively charged lysine) to maximize adhesion under varying conditions [61,62]. In applied contexts, catechol-based adhesives for carbon surfaces could be tuned by incorporating co-monomers that modulate the aromatic ring's electron density. For example, integrating aniline-like units (–NH_2 donors) or carboxylated phenyl units (–COOH acceptors) into a catechol-functionalized polymer may strengthen bonding to carbon fibers or graphitic fillers in composites.

Additionally, the pronounced effect of flexible alkyl linkers underscores the advantage of amphiphilic design in adhesive molecules. A hydrophobic tail allows the molecule to maximize van der Waals interactions by lying flat on a hydrophobic surface, while a polar catechol "head" anchors strongly through π interactions (and potentially covalent crosslinking if oxidized). This dual-mode interaction can be leveraged to achieve robust yet reversible noncovalent coupling between otherwise inert carbon surfaces and functional coatings. Overall, combining aromatic catechol units with flexible hydrophobic segments represents an effective strategy for adhesives targeting graphitic or other hydrophobic surfaces.

Another implication of our findings lies in electronics and sensing. For example, graphene-based electrodes or sensors could be functionalized with a thin catechol-derived layer to impart specific properties. Our results indicate that selecting appropriate substituents allows control not only of adhesion but also of the interfacial electronic characteristics through charge redistribution. Thus, beyond mechanical adhesion, the tunable interfacial charge redistribution identified here may influence the electronic environment at graphene or graphite interfaces.

To evaluate the possible influence of catechol oxidation, we also examined the adsorption of the corresponding quinone species on the graphite surface. The calculated adsorption energy of quinone is –62 $kJ{\cdot}mol^{-1}$, which is slightly more negative than that of catechol (–55 $kJ{\cdot}mol^{-1}$). This result suggests that oxidation does not necessarily weaken adsorption on graphitic surfaces. Although quinone lacks the catechol diol functionality, it still contains an aromatic ring that can interact with the graphitic π system, which is known to contribute significantly to catechol adsorption on graphite.

Finally, although the present calculations were performed in vacuum, it should be noted that mussel adhesion naturally occurs in aqueous environments. In wet environments, interfacial water molecules may influence adsorption in several ways. Water can form hydrogen bonds with polar functional groups such as –OH and –COOH, which may stabilize certain molecular conformations near the surface. In addition, solvent screening may partially reduce electrostatic interactions and interfacial dipoles, and solvation effects may influence the conformations of flexible side chains.

Previous theoretical studies have shown that catechol adsorption on hydrated graphite surfaces is still primarily governed by π–π interactions between the aromatic ring and the graphitic basal plane, while surrounding water molecules mainly interact with the adsorbed molecule through hydrogen bonding. For example, Chitumalla et al. reported that catechol adsorbs on wet graphite through π–π stacking with the graphite surface, and that water molecules further stabilize the adsorbed configuration via hydrogen bonding [63]. Therefore, although the absolute adsorption energies may vary in aqueous environments, the fundamental adsorption mechanism and the substituent-dependent trends identified in this work are expected to remain qualitatively similar under aqueous conditions.

4. Conclusions

This work uses first-principles calculations to investigate the adsorption of catechol and its derivatives on graphitic carbon surfaces. Catechol itself shows strong adsorption on graphite, with an adsorption energy of about –55 $kJ{\cdot}mol^{-1}$. Chemical functionalization of the aromatic ring further enhances adsorption: both electron-donating groups (e.g., –NH_2) and electron-withdrawing groups (e.g., –COOH) increase the adsorption strength relative to unsubstituted catechol, while the effect of substitution position (ortho vs. para) is comparatively minor. A more substantial increase in adsorption is achieved by introducing flexible alkyl linkers terminated with polar groups, which enlarge the effective contact area with the surface. Charge analysis further indicates that substituent polarity influences interfacial charge redistribution. Although the calculations were performed in vacuum to isolate intrinsic molecule–surface interactions, the trends identified here provide molecular-level guidelines for designing catechol-based molecules and polymers with improved affinity for graphitic and other hydrophobic surfaces.

CRediT authorship contribution statement

Mengdi Zhao: Writing – original draft, Software, Methodology. **Jinjin Zhang:** Formal analysis, Data curation. **Yanhong Yin:** Formal analysis. **Chunxian Guo:** Resources. **Joonkyung Jang:** Writing – review & editing, Conceptualization.

Declaration of competing interest

The authors declare that they have no known competing financial interests or personal relationships that could have appeared to influence the work reported in this paper.

Acknowledgments

This study was supported by the Natural Science Foundation of Jiangsu Province for Youths (BK20230662). Additional support was provided by the National Research Foundation of Korea (NRF) through a grant funded by the Korean government (MSIT) (No. 2021R1A2C1010936) and by the Korea Planning & Evaluation Institute of Industrial Technology, funded by the Korean government (Ministries of Trade, Industry, and Energy; Science and ICT; Interior and Safety; and the National Fire Agency) under the project "Development of Gas Hydrate Extinguishing Agent and Fire Suppression Technology for Inaccessible Fires" (Project No. 2760000002). This work was also supported by National Natural Science Foundation of China (22372113).

Data availability

Data will be made available on request.

References

[1] P. Huang, H. Zhang, H. Zeng, Mussel-inspired molecular strategies for fabricating functional materials with underwater adhesion and self-healing properties, Adv. Mater. 37 (2025) 2501542.
[2] Y.-Q. Wang, K.-C. Wang, Z. Liao, J.-Y. Ni, X.-L. Zhang, Y.-F. Li, Proteomic basis of mussel byssal adhesion: Substrate-specific expression of byssal proteins determines attachment performance, Int. J. Biol. Macromol. 332 (2025) 148592.
[3] S.X. Wang, J.H. Waite, Catechol redox maintenance in mussel adhesion, Nat. Rev. Chem. 9 (2025) 159–172.
[4] A. Shrestha, K. Kojio, Y. Shiota, S. Yamamoto, K. Tanaka, K. Satoh, K. Yoshizawa, A DFT study of catechol polymer adhesion onto γ-alumina (110) surfaces, Langmuir 41 (2025) 23672–23687.
[5] I.-C. Yeh, J.L. Lenhart, J.A. Orlicki, B.C. Rinderspacher, Molecular dynamics simulation study of adsorption of bioinspired oligomers on alumina surfaces, J. Phys. Chem. B 123 (2019) 7024–7035.
[6] J. Yu, Y. Kan, M. Rapp, E. Danner, W. Wei, S. Das, D.R. Miller, Y. Chen, J.H. Waite, J.N. Israelachvili, Adaptive hydrophobic and hydrophilic interactions of mussel foot proteins with organic thin films, Proc. Natl. Acad. Sci. 110 (2013) 15680–15685.
[7] S. Jee, M. Rammal, T. Priemel, D.S. Bohle, M.J. Harrington, Vanadium uptake and storage in the fabrication and function of mussel byssus, New J. Chem. 48 (2024) 16177–16188.

[8] T. Priemel, G. Palia, F. Förste, F. Jehle, S. Sviben, I. Mantouvalou, P. Zaslansky, L. Bertinetti, M.J. Harrington, Microfluidic-like fabrication of metal ion-cured bioadhesives by mussels, Science 374 (2021) (1979) 206–211.
[9] M. Mesko, L. Xiang, S. Bohle, D.S. Hwang, H. Zeng, M.J. Harrington, Catechol-vanadium binding enhances cross-linking and mechanics of a mussel byssus coating protein, Chem. Mater. 33 (2021) 6530–6540.
[10] G.-Q. Pan, B. Li, A dynamic biointerface controls mussel adhesion, Science 382 (2023) 763–764.
[11] P. Chen, Y. Zhang, P. Zhang, X. Zhao, Y. Wu, Mussel-inspired catechol prepolymers as surface primer for enhanced interface bonding to high-performance thermoplastics, Polymer (Guildf). 307 (2024) 127254.
[12] S. Valappil, M.C.D. Madhav, S.S. Raghavan, A. Nagaraj, S. Easwaramoorthi, S. Vijayavenkataraman, G. Ponesakki, A. Niraikulam, Mussel foot protein with genetically incorporated hydroxyproline and DOPA exhibits enhanced phase separation and underwater adhesion, Int. J. Biol. Macromol. 322 (2025) 146609.
[13] K. Carter-Fenk, M. Liu, L. Pujal, M. Loipersberger, M. Tsanai, R.M. Vernon, J. D. Forman-Kay, M. Head-Gordon, F. Heidar-Zadeh, T. Head-Gordon, The energetic origins of pi–pi contacts in proteins, J. Am. Chem. Soc. 145 (2023) 24836–24851.
[14] S. Xu, M. Kang, X. Xin, J. Liang, H. Xiao, Y. Lu, J. Yang, H. Zhai, Design principles and application research of mussel-inspired materials: a review, J. Environ. Chem. Eng. 12 (2024) 111655.
[15] Y.-S. Liu, Y. Li, W.-Y. Su, T.-H. Jian, C.-T. Kao, Y.-Y. Tsai, C.-J. Tsai, A. Thyparambil, Y. Wei, Uncovering mussel foot protein (Mfp-3)'s binding secrets: Enhanced biomimetic adhesives via mass spectrometry and residue labeling, Colloids Surf. A Physicochem. Eng. Asp. 702 (2024) 134953.
[16] Y. Tsuji, Y. Kitamura, M. Someya, T. Takano, M. Yaginuma, K. Nakanishi, K. Yoshizawa, Adhesion of epoxy resin with hexagonal boron nitride and graphite, ACS Omega 4 (2019) 4491–4504.
[17] Y. Wu, X. Zhang, C. Liu, L. Tian, Y. Zhang, M. Zhu, W. Qiao, J. Wu, S. Yan, H. Zhang, Adsorption behaviors and mechanism of phenol and catechol in wastewater by magnetic graphene oxides: a comprehensive study based on adsorption experiments, mathematical models, and molecular simulations, ACS Omega 9 (2024) 15101–15113.
[18] Y. Li, M. Liao, J. Zhou, Catechol and its derivatives adhesion on graphene: insights from molecular dynamics simulations, J. Phys. Chem. C 122 (2018) 22965–22974.
[19] S. Vuppala, R.K. Chitumalla, S. Choi, T. Kim, H. Park, J. Jang, Machine learning-assisted computational screening of adhesive molecules derived from dihydroxyphenyl alanine, ACS Omega 9 (2023) 994–1000.
[20] A. Barua, M.S. Rahman, A. Sannyal, M.S. Khan, S. Faraezi, Interfacial structure and dynamics of dihydroxybenzene isomers influenced by the inter-intra molecular interaction of substituents, Comput. Theor. Chem. 1220 (2023) 113979.
[21] A. BiBi, S. Sayadi, M. Abu-Dieyeh, N. Zouari, M.A. Al-Ghouti, Adsorption of phenol and bisphenol-A by activated carbon and graphene oxide: a comparative study, Environ. Sci. Pollut. Res. 32 (2025) 28840–28863.
[22] D. Lin, B. Xing, Adsorption of phenolic compounds by carbon nanotubes: role of aromaticity and substitution of hydroxyl groups, Environ. Sci. Technol. 42 (2008) 7254–7259.
[23] V. Subasinghege Don, L. Kim, R. David, J.A. Nauman, R. Kumar, Adsorption studies at the graphene oxide–liquid interface: a molecular dynamics study, J. Phys. Chem. C 127 (2023) 5920–5930.
[24] A. Rochefort, J.D. Wuest, Interaction of substituted aromatic compounds with graphene, Langmuir 25 (2009) 210–215.
[25] M. Orio, D.A. Pantazis, F. Neese, Density functional theory, Photosynth. Res. 102 (2009) 443–453.
[26] K. Burke, Perspective on density functional theory, J. Chem. Phys. 136 (2012) 150901.
[27] J. Hafner, Ab-initio simulations of materials using VASP: Density-functional theory and beyond, J. Comput. Chem. 29 (2008) 2044–2078.
[28] J. Hafner, Materials simulations using VASP—a quantum perspective to materials science, Comput. Phys. Commun. 177 (2007) 6–13.
[29] B. Hammer, L.B. Hansen, J.K. Nørskov, Improved adsorption energetics within density-functional theory using revised Perdew-Burke-Ernzerhof functionals, Phys. Rev. B 59 (1999) 7413.
[30] X. Xu, W.A. Goddard III, The extended Perdew-Burke-Ernzerhof functional with improved accuracy for thermodynamic and electronic properties of molecular systems, J. Chem. Phys. 121 (2004) 4068–4082.
[31] Y. Gogotsi, J.A. Libera, N. Kalashnikov, M. Yoshimura, Graphite polyhedral crystals, Science 290 (2000) (1979) 317–320.
[32] H.S. Lipson, A.R. Stokes, The structure of graphite, Proc. R. Soc. Lond. A Math. Phys. Sci. 181 (1942) 101–105.
[33] J.C. Chacon-Torres, L. Wirtz, T. Pichler, Manifestation of charged and strained graphene layers in the Raman response of graphite intercalation compounds, ACS Nano 7 (2013) 9249–9259.
[34] H. Tang, Y. Zhao, S. Shan, X. Yang, D. Liu, F. Cui, B. Xing, Theoretical insight into the adsorption of aromatic compounds on graphene oxide, Environ. Sci. Nano 5 (2018) 2357–2367.
[35] K. Spyrou, M. Calvaresi, E.K. Diamanti, T. Tsoufis, D. Gournis, P. Rudolf, F. Zerbetto, Graphite oxide and aromatic amines: size matters, Adv. Funct. Mater. 25 (2015) 263–269.
[36] Q. Jia, C. Yang, B.J. Venton, K.H. DuBay, Atomistic simulations of dopamine diffusion dynamics on a pristine graphene surface, ChemPhysChem 23 (2022) e202100783.
[37] L.M. Cam, L. Van Khu, N.N. Ha, Theoretical study on the adsorption of phenol on activated carbon using density functional theory, J. Mol. Model. 19 (2013) 4395–4402.
[38] A. Supong, U.B. Sinha, D. Sinha, Density functional theory calculations of the effect of oxygenated functionals on activated carbon towards cresol adsorption, Surfaces 5 (2022) 280–289.
[39] J. Lim, S. Zhang, J.-M. Heo, M.C. Dickwella Widanage, A. Ramamoorthy, J. Kim, Polydopamine adhesion: catechol, amine, dihydroxyindole, and aggregation dynamics, ACS Appl. Mater. Interfaces 16 (2024) 31864–31872.
[40] Q. Wu, B. Xiao, Y. Li, R. Yao, D. Jin, Y. Lei, D. Yang, J. Zhu, Bioactive chitosan/polydopamine nanospheres coating on carbon fiber towards strengthening epoxy composites, Int. J. Biol. Macromol. 275 (2024) 133568.
[41] B.K. Ahn, Perspectives on mussel-inspired wet adhesion, J. Am. Chem. Soc. 139 (2017) 10166–10171.
[42] J. Yu, W. Wei, M.S. Menyo, A. Masic, J.H. Waite, J.N. Israelachvili, Adhesion of mussel foot protein-3 to TiO2 surfaces: the effect of pH, Biomacromolecules 14 (2013) 1072–1077.
[43] T. Utzig, P. Stock, M. Valtiner, Resolving non-specific and specific adhesive interactions of catechols at solid/liquid interfaces at the molecular scale, Angew. Chem. Int. Ed. 55 (2016) 9524–9528.
[44] W. Wei, J. Yu, C. Broomell, J.N. Israelachvili, J.H. Waite, Hydrophobic enhancement of dopa-mediated adhesion in a mussel foot protein, J. Am. Chem. Soc. 135 (2013) 377–383.
[45] M.S. Desai, M. Chen, F.H.J. Hong, J.H. Lee, Y. Wu, S.-W. Lee, Catechol-functionalized elastin-like polypeptides as tissue adhesives, Biomacromolecules 21 (2020) 2938–2948.
[46] T. Frederiksen, C. Munuera, C. Ocal, M. Brandbyge, M. Paulsson, D. Sánchez-Portal, A. Arnau, Exploring the tilt-angle dependence of electron tunneling across molecular junctions of self-assembled alkanethiols, ACS Nano 3 (2009) 2073–2080.
[47] E. Mete, M. Yortanlı, M.F. Danışman, A van der Waals DFT study of chain length dependence of alkanethiol adsorption on Au (111): physisorption vs. chemisorption, PCCP 19 (2017) 13756–13766.
[48] O. Yaffe, Y. Qi, L. Scheres, S.R. Puniredd, L. Segev, T. Ely, H. Haick, H. Zuilhof, A. Vilan, L. Kronik, Charge transport across metal/molecular (alkyl) monolayer-Si junctions is dominated by the LUMO level, Phys. Rev. B—Condensed Matter Mater. Phys. 85 (2012) 045433.
[49] L. Belding, S.E. Root, Y. Li, J. Park, M. Baghbanzadeh, E. Rojas, P.F. Pieters, H. J. Yoon, G.M. Whitesides, Conformation, and charge tunneling through molecules in SAMs, J. Am. Chem. Soc. 143 (2021) 3481–3493.
[50] Y. Liu, X. Qiu, S. Soni, R.C. Chiechi, Charge transport through molecular ensembles: recent progress in molecular electronics, Chem. Phys. Rev. 2 (2021) 021303.
[51] A. Salomon, T. Boecking, O. Seitz, T. Markus, F. Amy, C. Chan, W. Zhao, D. Cahen, A. Kahn, What is the barrier for tunneling through alkyl monolayers? Results from n-and p-Si-alkyl/Hg junctions, Adv. Mater. 19 (2007) 445–450.
[52] X. Chen, B. Kretz, F. Adoah, C. Nickle, X. Chi, X. Yu, E. Del Barco, D. Thompson, D. A. Egger, C.A. Nijhuis, A single atom change turns insulating saturated wires into molecular conductors, Nat. Commun. 12 (2021) 3432.
[53] B. Das, R. Voggu, C.S. Rout, C.N.R. Rao, Changes in the electronic structure and properties of graphene induced by molecular charge-transfer, Chem. Commun. 41 (2008) 5155–5157.
[54] M. Shakourian-Fard, Z. Jamshidi, G. Kamath, Surface charge-transfer doping of graphene nanoflakes containing double-vacancy (5-8-5) and stone-wales (55-77) defects through molecular adsorption, ChemPhysChem 17 (2016) 3289–3299.
[55] O. Leenaerts, B. Partoens, F.M. Peeters, Paramagnetic adsorbates on graphene: a charge transfer analysis, Appl. Phys. Lett. 92 (2008) 243125.
[56] Y. Mo, J. Gao, Polarization and charge-transfer effects in Lewis Acid- Base complexes, J. Phys. Chem. A 105 (2001) 6530–6536.
[57] Y. Zhang, X. Chen, D. Fang, H. Yan, D. Wang, X. Wang, J. Li, Y. Zhai, X. Chu, D. Wang, Adsorption behavior of NO and NO_2 on two-dimensional As, Sb, and Bi materials: first-principles insights, Materials 17 (2024) 1024.
[58] S. Das, N.R.M. Rodriguez, W. Wei, J.H. Waite, J.N. Israelachvili, Peptide length and dopa determine iron-mediated cohesion of mussel foot proteins, Adv. Funct. Mater. 25 (2015) 5840–5847.
[59] S.-B. Lee, C. González-Cabezas, K.-M. Kim, K.-N. Kim, K. Kuroda, Catechol-functionalized synthetic polymer as a dental adhesive to contaminated dentin surface for a composite restoration, Biomacromolecules 16 (2015) 2265–2275.
[60] J. Ren, R. Kong, H. Wang, S. Du, P. Liu, H. Wang, Y. Chen, G. Xie, L. Zhang, J. Zhu, Robust underwater adhesion of catechol-functionalized polymer triggered by water exchange, Small Methods 7 (2023) 2201235.
[61] G.P. Maier, C.M. Bernt, A. Butler, Catechol oxidation: considerations in the design of wet adhesive materials, Biomater. Sci. 6 (2018) 332–339.
[62] Y. Li, J. Cheng, P. Delparastan, H. Wang, S.J. Sigg, K.G. DeFrates, Y. Cao, P. B. Messersmith, Molecular design principles of Lysine-DOPA wet adhesion, Nat. Commun. 11 (2020) 3895.
[63] R.K. Chitumalla, K. Kim, X. Gao, J. Jang, A density functional theory study on the underwater adhesion of catechol onto a graphite surface, PCCP 23 (2021) 1031–1037.